

Final Draft
of the original manuscript:

Bäckemo, J.; Heuchel, M.; Reinthaler, M.; Kratz, K.; Lendlein, A.:
**Predictive topography impact model for Electrical Discharge Machining
(EDM) of metal surfaces.**

In: MRS Advances . Vol. 5 (2020) 12 - 13, 621-632.

First published online by Cambridge University Press: 18.11.2019

DOI: 10.1557/adv.2019.433

<https://dx.doi.org/10.1557/adv.2019.433>

Predictive topography impact model for Electrical Discharge Machining (EDM) of metal surfaces

Johan Bäckemo^{1,2}, Matthias Heuchel¹, Markus Reinthaler^{1,3}, Karl Kratz¹, and Andreas Lendlein^{1,2,*}

1. Institute of Biomaterial Research and Berlin-Brandenburg Center for Regenerative Therapies, Helmholtz-Zentrum Geesthacht, Kantstrasse 55, 14513 Teltow, Germany
2. Institute of Chemistry, University of Potsdam, Karl-Liebknecht-Str. 24/25, 14476 Potsdam, Germany
3. Department of Cardiology, Campus Benjamin Franklin, Charité Berlin, Berlin, Germany

* To whom correspondence should be addressed:

Prof. Dr. Andreas Lendlein, email: andreas.lendlein@hzg.de

ABSTRACT

Electrical discharge machining (EDM) is a method capable of modifying the microstructure of metal surfaces. Here, we present a predictive computer supported model of the roughness generated on the surface by this process. EDM is a stochastic process, in which charge generated between a metallic substrate and an electrode creates impacts, and thus is suitable for modeling through iterative simulations. The resulting virtual, modified surface structures were evaluated for roughness. Curvatures were analyzed using Abbott-Firestone curves. Three radii of impacts (10, 20, 30 μm) and two values for the depth to radius ratio (0.1, 0.3) were used as input parameters to compute a total of six simulations. It was found that the roughness parameters followed an inverse exponential trend as a function of impact number, and that the strongly concave curvatures reached equilibrium at an earlier impact number for lower depth to radius ratios.

INTRODUCTION

Electrical Discharge Machining (EDM) is a process in which a metallic substrate is brought into close vicinity with an electrode and subjected to repeated sparks, which iteratively removes material – ultimately creating a rough surface [1]. This process is commonly used for difficult-to-machine materials, tooling of complex parts and especially highly accurate micro parts [2]. The roughness of the surface is dependent on many variables such as electrical parameters (voltage, pulse duration, and dielectric influence [3]) and duration of treatment. EDM is a random process, and a probable statistical distribution governs the geometrical parameters and must be taken into account – but as a first approximation the parameters were fixed for each impact for a given simulation. The size of each individual impact is dependent on the charge built up before each spark [3] which is a function of the said electrical parameters, and the number of sparks is dependent on the duration of treatment. Thus, the size of impact and duration of treatment were considered for simulation in this paper. It is of interest to researchers who wish to create surfaces with not only a specific roughness profile, but also a curvature profile. It has previously been discussed that to determine fatigue limits for milled surfaces roughness parameters are not sufficient but that curvature parameters show good correlation for this application [4]. For this purpose, it would be important to see how these parameters differ with each iteration, i.e. impact from spark. Our aim is to get a better understanding for how this iterative process changes the surface topographically with respect to processing time, and that we can relate the output parameters of roughness and curvature to the input parameters. Thus, our hypothesis is that this kind of process could be modeled by an iterative approach, where each iteration subjects the surface to an additional impact from a spark. The motivation and purpose for this study is to be able to manufacture surfaces with defined topographical parameters that are later intended for technical (e.g. aerospace materials [5]) or medical applications, such as orthopedic and dental implant surfaces [6] – and to be able to anticipate these parameters by means of simulation

Considering there is no preference for the location of each impact it can be assumed that this process is stochastic. To model this process by using randomly chosen points on a surface would therefore be suitable. In order predict how surfaces topographically change with each impact, it may be of interest to look at how roughness and curvature changes throughout the process. More importantly, a salient point would be to determine if, at a certain number of iterations, these output parameters reach an equilibrium and do not significantly change with subsequent impacts.

METHODS

Model

The generation of a crater with a surrounding rim by a combined spherical cap and half-torus is modeled, as shown in Fig. 1 (A-B). The model used for calculating the deformation was assumed to be ellipsoidal in a previous report [7], however such craters of a concave bowl with bulging rim have been found in simulation studies of simple spark impacts considering both heating and material ejection [8,9]. The spherical cap creates a crater and the torus creates a ridge. The grey line shows the surface datum line, which is initially a flat plane. A point is chosen on that line, which is the point of impact. The points that fall within the region of the inner and outer circles are deformed accordingly. Overlapping behavior was also considered. It was assumed that a ridge would be formed for each impact due to the physical removal of material for an EDM process, i.e. a ridge could be formed inside of the crater from a previous impact. For each iteration, the volume

(V) was calculated and removed and a fraction thereof, F , was used to build the ridge (see equations 1-4). F was set to 0.5 as preliminary results from visual inspection of an actual EDM-treated surface indicated that this may be a good first approximation (see Figure). It has previously been shown that electrical discharge energy has a direct influence on average diameter and maximum depth, and that the relationship appears to follow a logarithmic trend [7]. Bartkowiak and Brown also showed that surface discharge energy influences curvature calculation strongly at smaller scales, but showed little variance at larger scales [10]. Others have also reported that crater size increases with increasing current supplied to the EDM [11].

The model was applied to an initially flat surface measuring 1000 x 1000 points with a distance of 1 μm in between each point. The simulation ran iteratively up to 10,000 impacts. Two input parameters were used to determine the extent of changing surface parameters on the surface: radius of impact a , and the ratio between h and a . The values chosen for a were fixed to 10, 20, and 30 μm , and for the h/a ratio, 0.1 and 0.3, and were kept constant for each simulation. The radius of the ridge formed were calculated as 2, 4, 6 μm for each value of a . Equations (1)-(4) give the relation between the model parameters (a , h , F) and the crater radius and respective volume calculations.

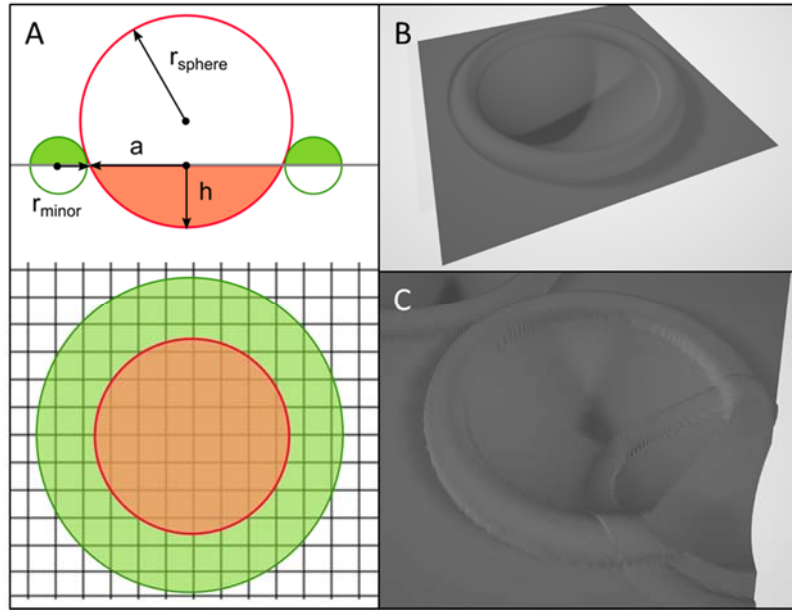


Figure 1 Schematic of combined spherical cap and torus model used for iterative deformation of a metallic surface. A) Top: Side view of deformation model, showing areas that are deformed below datum line (larger circle) and above datum line (smaller outer circles). Bottom: Top view of deformation model show areas that are deformed below datum line (inner circle) and above datum line (outer circle). B) 3D-rendering of a single impact. C) 3D-rendering highlighting overlapping behavior.

$$r_{sphere} = \frac{a^2 + h^2}{2h} \quad (1)$$

$$V_{spherical\ cap} = \frac{1}{6}\pi h(3a^2 + h^2) \quad (2)$$

$$V_{halftorus} = \pi^2 R r_{minor}^2 = \pi^2 (a + r_{minor}) r_{minor}^2 \quad (3)$$

$$V_{torus} = F \cdot V_{spherical\ cap} \quad (4)$$

Roughness of the initially flat surface was calculated after a certain number of random impacts. Curvatures were also analyzed for the modified virtual surface.

Roughness evaluation

Roughness parameters were calculated based on the Abbott-Firestone curve for a 2D-surface, as defined by the standard ISO 25178 [12]. Initially the probability density function (PDF) of the material proportion was calculated, and by drawing a tangential line at 40% cumulative material proportion [13], the roughness parameters Sk , Spk , Svk , $Smr1$ and $Smr2$ were calculated (Table 1).

Table 1 – Surface roughness parameters obtained from an Abbott-Firestone curve, defined by ISO 25178

Parameter	Description
Sk	Surface roughness core profile
Spk	Reduced peak roughness
Svk	Reduced valley roughness
$Smr1$	Upper material portion
$Smr2$	Lower material portion

For each iteration, i.e. each impact, an Abbott-Firestone curve was computed and surface roughness parameters were evaluated each decade with intermediate steps 2 and 5, e.g. 1, 2, 5, 10, 20...5 000, 10 000. The changes in these parameters at these intervals were then analyzed.

Curvature evaluation

Previous reports have calculated the curvatures of a surface in terms of principal curvatures at different scales, such e.g. in [10]. Here, curvature is described as a second order tensor, which is based on the work by Weingarten [14]. The principal, Gaussian and average curvature values can be determined for each point from this tensor. However for this study, not only the principal curvatures are of interest but also the curvatures at a particular point in all directions. For any given point, N number of directions were chosen to analyze curvature. For each direction three points were chosen: the given point, a point L units away in the given direction, and a point L units away in the opposite direction. With these three points, one can define a circle on a 2D-plane (See Fig. 2). This method is similar to the procedure reported in [15], where calculations are based on Heron's formula.

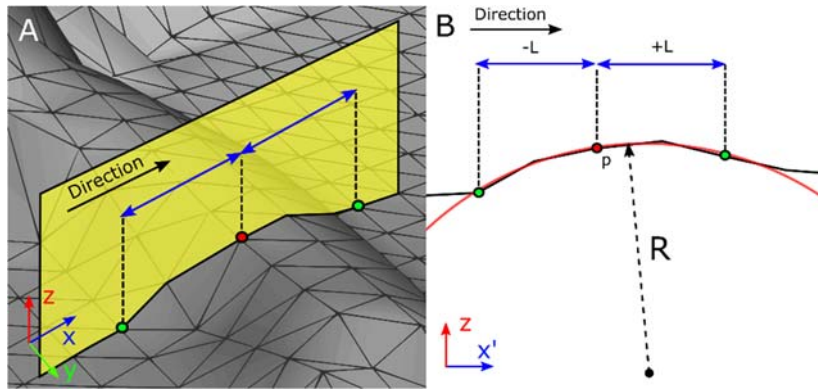


Figure 2 – Schematic of calculating curvature using 3 points on a 2D-plane and inscribing a circle on to it. For any three points $\in \mathbb{R}^2$ there is only one unique solution to fit a circle. A) Looking at the selected points from the surface. B) Look at the selected points at the cut plane.

Once the coordinates of this set of three points are given, one can inscribe a circle using the steps below.

The three points are defined as:

$$p_1 = (x'_1, z_1), p_2 = (x'_2, z_2), p_3 = (x'_3, z_3)$$

The equation of a circle is described by the equation:

$$Ax'^2 + Az^2 + Bx' + Cz + D = 0$$

Substituting the three points, which lie on the circle, a system of equations is obtained which can be described by the determinant.

$$\begin{vmatrix} x'^2 + z^2 & x' & z & 1 \\ x'^2_1 + z^2_1 & x'_1 & z_1 & 1 \\ x'^2_2 + z^2_2 & x'_2 & z_2 & 1 \\ x'^2_3 + z^2_3 & x'_3 & z_3 & 1 \end{vmatrix} = 0$$

Where,

$$A = \begin{vmatrix} x'_1 & z_1 & 1 \\ x'_2 & z_2 & 1 \\ x'_3 & z_3 & 1 \end{vmatrix}, B = - \begin{vmatrix} x'^2_1 + z^2_1 & z_1 & 1 \\ x'^2_2 + z^2_2 & z_2 & 1 \\ x'^2_3 + z^2_3 & z_3 & 1 \end{vmatrix},$$

$$C = \begin{vmatrix} x'^2_1 + z^2_1 & x'_1 & 1 \\ x'^2_2 + z^2_2 & x'_2 & 1 \\ x'^2_3 + z^2_3 & x'_3 & 1 \end{vmatrix}, D = - \begin{vmatrix} x'^2_1 + z^2_1 & x'_1 & z_1 \\ x'^2_2 + z^2_2 & x'_2 & z_2 \\ x'^2_3 + z^2_3 & x'_3 & z_3 \end{vmatrix}$$

$$r = \sqrt{(x' - x'_1)^2 + (z - z_1)^2} = \sqrt{\frac{B^2 + C^2 - 4AD}{4A^2}}$$

$$K = \frac{1}{r}$$

By taking the inverse of the radius of that circle one determines the curvature in this particular direction. For this analysis L was set to 30 μm . This was repeated for each direction. The number of directions was determined by rotating around the z-axis at the point - 10 degrees for each direction - thus a total of 36 directions. Due to symmetry of the three-point circle calculation, this was reduced to a total of 18 directions. Each point on the surface was evaluated in this manner.

Similar to evaluating the roughness of the surface by computing an analogue to an “Abbott-Firestone” curve, the same principle could be extrapolated to evaluating curvature. Thus curvature parameters for the whole surface were defined, based on the roughness analysis (

Table 2). Concavity and convexity refers to positive and negative curvature respectively.

Table 2 – Proposed curvature parameters

Parameter	Description
<i>Kk</i>	Surface curvature core profile
<i>Kpk</i>	Reduced concavity curvature
<i>Kvk</i>	Reduced convexity curvature
<i>Kmr1</i>	Upper material portion
<i>Kmr2</i>	Lower material portion

RESULTS AND DISCUSSION

EDM-treated surface and simulated surface comparison

Initial tests of the suitability of the model consisted of comparing a modelled surface with a stainless steel EDM-treated surface (Fig. 3). From the EDM-treated surface, one can clearly see the formation of craters with neighboring ridges. What can also be noted, is that the impact craters appear similar in size and shape. Compared to the simulated surface one can see a clear similarity, and the overlapping behavior from subsequent impacts also are present in the EDM-treated surface. Thus the proposed model was deemed suitable to describe the topographical shape of an EDM-surface.

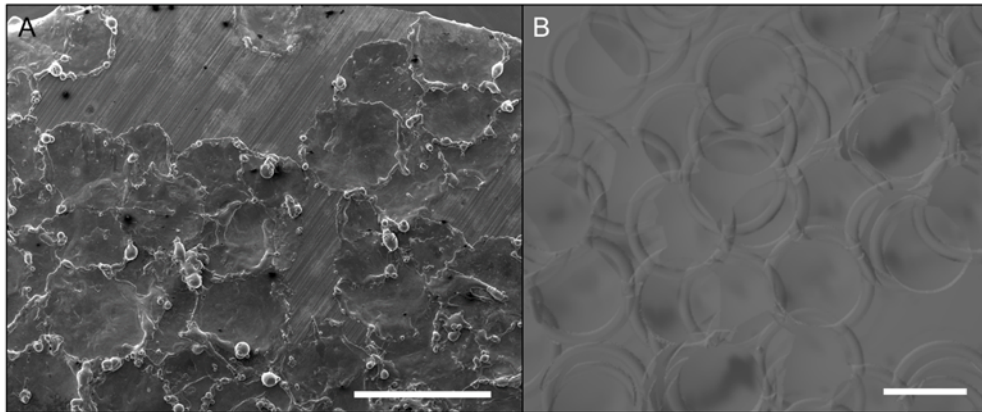


Figure 3 – A) A Scanning Electron Microscopy (SEM) image of a stainless steel EDM treated surface. Scale bar = 1000 μm . B) A surface generated from simulation. Scale bar = 30 μm

Roughness and Curvature analysis

Roughness and curvature analysis were performed after $n = 1, 2, 5, 10, 20, 50, 100, 200, 500, 1000, 2000, 5000, 10000$ impacts to allow logarithmic plot of the results. The Abbott-Firestone curves for roughness and curvature differ somewhat in shape (Fig. 4). For the roughness analysis, the Abbott-Firestone has a sigmoid shape, as expected, in which the different areas of Sk , Spk , and Svk are also clearly defined. For the proposed curvature analysis, the Abbott-Firestone has a much sharper appearance, with a plateau in the middle, creating a horizontal tangential line. In addition, the upper and lower material parts are greater for the curvature analysis than for the roughness analysis. This is expected as there are mainly two radii on the surface, that of the crater, a , and that of the ridge, r_{minor} . For a value of $a = 30 \mu\text{m}$, the expected curvature from the center going out radially would be $0.033 \mu\text{m}^{-1}$, and for a value of $r_{\text{minor}} = 6 \mu\text{m}$ a curvature of $0.16 \mu\text{m}^{-1}$. However there are values out of these regions which can be explained that there are directions that go in all directions, thus if one looks at a point in the crater off-center then the expected curvature values in all directions should differ.

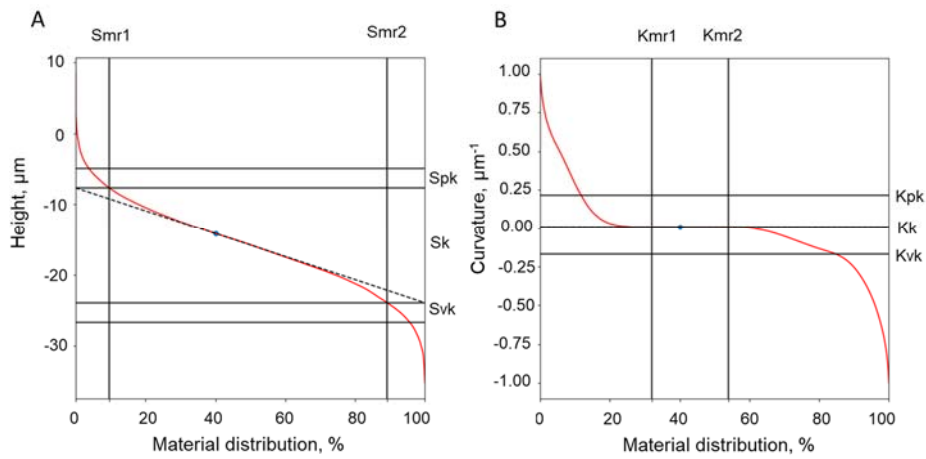


Figure 4. Abbott-Firestone roughness and curvature curves from a surface with the input $a = 30 \mu\text{m}$ and $h/a = 0.1$ after 5000 random impacts. The point at 40% material distribution shows at what point the tangential line is drawn, this in turn defined the parameter Sk and Kk . A) Abbott-Firestone roughness curve. B) Abbott-Firestone curvature curve

In the interest of predictive modeling, one should try to answer the question of how long a treatment should be conducted to reach a certain roughness value. By looking how the parameters change over time it may give further insight on how to fine tune the input parameters in order to reach the desired properties. For the roughness parameters the core roughness profile, Sk , gives information of how much the overall roughness changes with each impact, whereas the reduced peak height shows how the number of peaks above the core profile changes with each impact. These graphs are depicted in Fig. 3. From these graphs, it is apparent that Sk initially changes rapidly and stabilizes with increasing number of impacts. This would mean that after 10,000 impacts the surface does not change significantly. Spk seems to follow the same trend. Comparing the top and bottom graphs, one sees that the values for both Sk and Spk are greater for $h/a = 0.3$, which is logical seeing that the depth is greater, and thus for each impact a greater height difference is achieved.

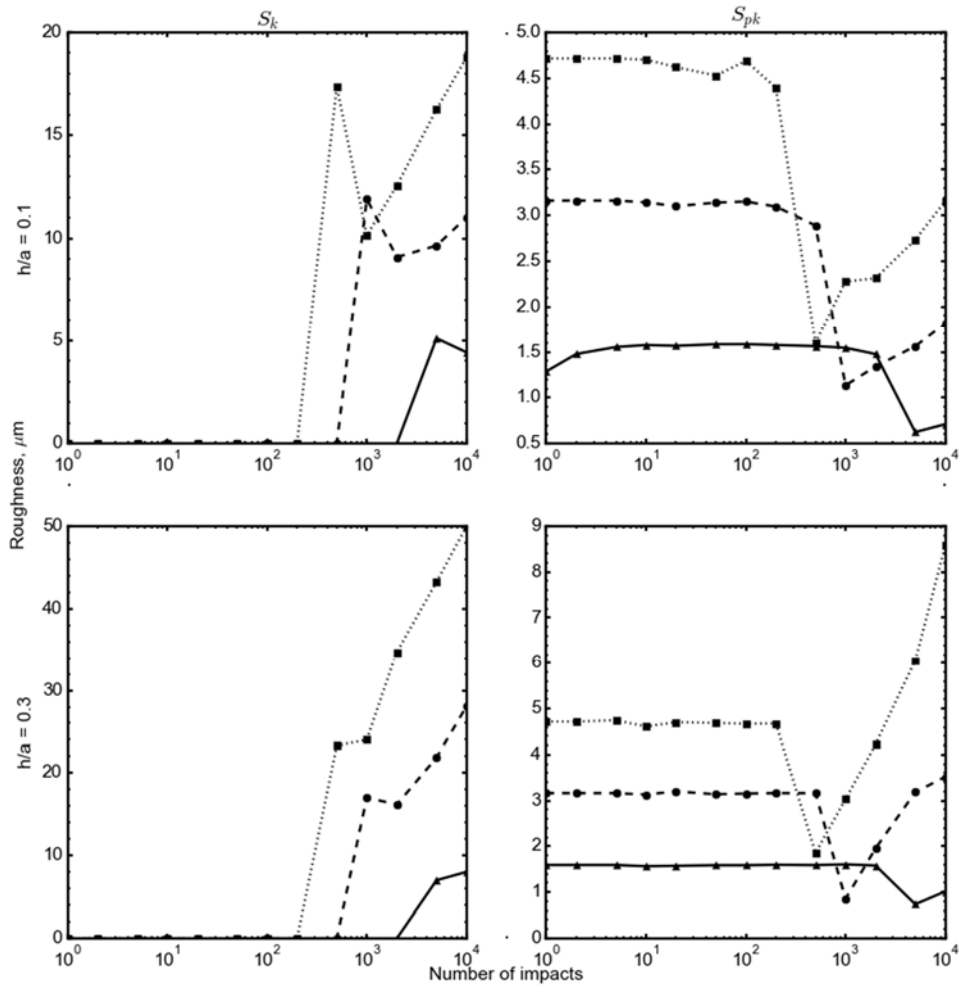


Figure 5 – Graphs of plotting S_k , core roughness profile (left), and S_{pk} , reduced peak height (right), as a function of number of impacts. Graphs with $h/a = 0.1$ (top), $h/a = 0.3$ (bottom). Lines are shown for impact radius, a , of $10\ \mu\text{m}$ (line), $20\ \mu\text{m}$ (dashed), and $30\ \mu\text{m}$ (dotted).

On the other hand, there is an apparent difference between the curvature results (see Fig. 5). The core curvature profile appears to increase greatly during the initial phase of impacts, and then switch sporadically from low to high. In contrast, the reduced concavity profile, Kpk , steadily increases until it reaches a final value and plateaus. Also of note, is that the value of Kpk is inversely proportional to a , since curvature is defined as the reciprocal of the radius of a circle. For any value of a , Kpk reaches an equilibrium plateau after a certain number of impacts, which could be due to the curvature values present on the surface are related to a , and after a certain number of impacts all points on the surface have been deformed at least once, and thus the curvature profile does not change significantly due to subsequent impacts. What can also be seen is that the greater

the value of a , the quicker the surface reaches its final Kpk value, which may be explained by the fact that the proportion of the surface deformed with respect to the total surface increases. Comparing the lower and upper graphs, one can see that Kpk appears to reach equilibrium at a later impact number for $h/a = 0.3$ compared to $h/a = 0.1$, this most notably seen for $a = 10 \mu\text{m}$.

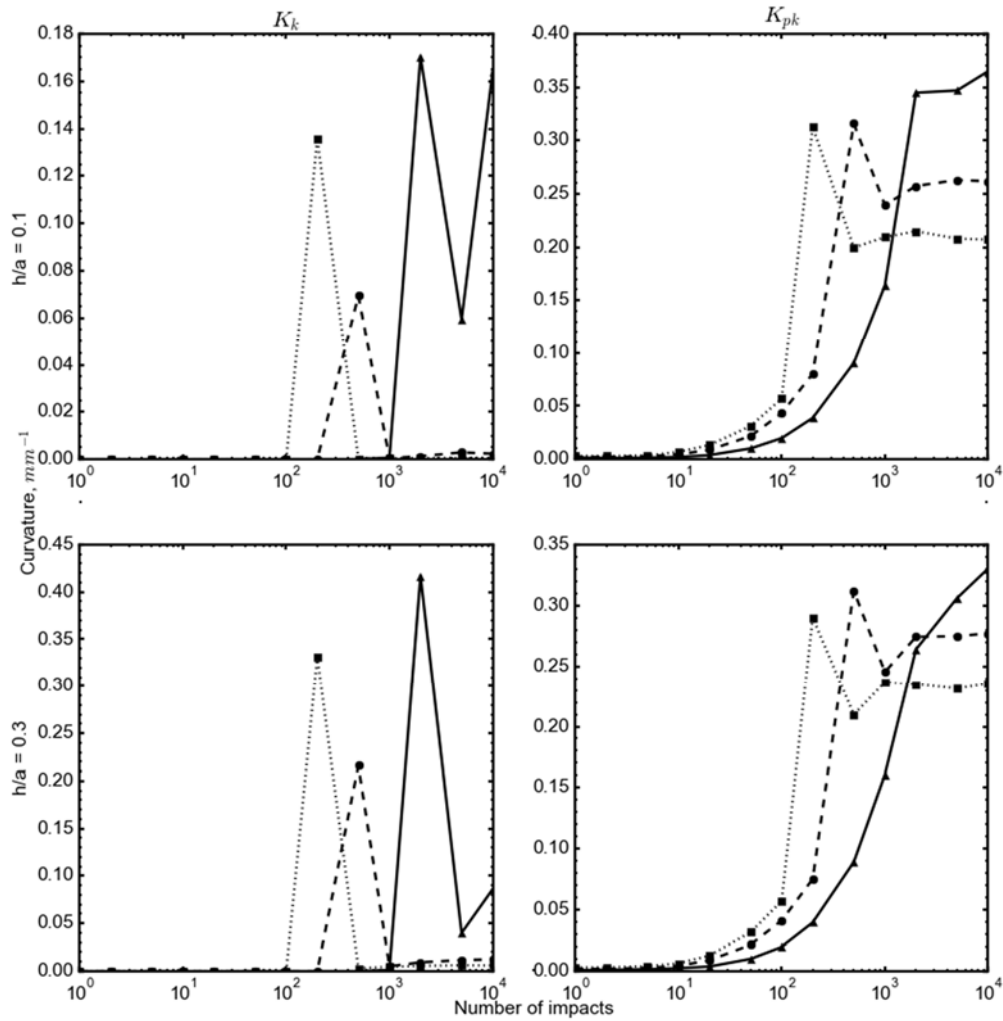


Figure 6 - Graphs of plotting K_k , core curvature profile (left), and K_{pk} , reduced curvature concavity profile (right), as a function of number of impacts. Graphs with $h/a = 0.1$ (top), $h/a = 0.3$ (bottom). Lines are shown for impact radius, a , of $10 \mu\text{m}$ (line), $20 \mu\text{m}$ (dashed), and $30 \mu\text{m}$ (dotted).

The values for Sk as a function of impact number appears to follow an inverse exponential trend, which could be explained by that given that the process is stochastic. The probability of extreme height differences between the lowest and highest point is small

– meaning that the roughness would tend to approach an asymptote at a particular roughness value. For a given impact radius, a , the strongly concave curvatures will reach its final value at an earlier impact number for a high h/a ratio compared to a lower one. In addition, a flat surface has no curvature by definition – but at a certain impact number all points are deformed, and each point will have non-zero curvature in all directions. This may seem contrary to the Abbott-Firestone curvature curve (Fig. 4B) as it appears to be a plateau at around $0 \mu\text{m}^{-1}$, however these points are in fact weakly concave or convex. This weak concavity and convexity may come from the points on the ridges where the some directions are tangential to the ridges, which are weakly concave. The same is true for the off-centre points in the craters.

In this work, a length of $30 \mu\text{m}$ was selected to define three points in order to define the curvature for a given point in a given direction. Changing the value of this length will have a direct impact on the curvature calculation and on the “Abbott-Firestone” curves. In our future work we will consider multi-scale curvature analysis [4, 14] and further topographical analysis [16].

It can be assumed from a comparing real and computed surfaces in Fig. 6 that the formation of globules in the real surface is not replicated in the simulated surface. This was omitted, since the modelling of such a variant structure needs more careful analysis of the sizes of such globules, similar to the method reported in [11].

CONCLUSION

In this study the EDM process was modeled using a combined spherical cap and torus model which was deemed suitable for the purposes of fabrication design by comparing the results to an EDM-treated stainless steel surface. As the surface underwent this treatment as function of impact number, its Sk value followed an inverse exponential trend, which was as expected due to its stochastic nature. Furthermore, it was shown that one can control the strongly concave and strongly convex regions by reaching a certain impact number, however more simulations are needed in order to define the core curvature profile through varying more input parameters.

ACKNOWLEDGEMENTS

This work was financially supported by the Helmholtz-Association of German Research Centers (through program-oriented funding, and through the Helmholtz Graduate School of Macromolecular Bioscience [MacroBio], grant no. VH-GS-503).

REFERENCES

- [1] S. Kumar, R. Singh, T.P. Singh, and B.L. Sethi, *J. Mater. Process. Technol.* **209**, 3675 (2009).
- [2] M. Gostimirovic, P. Kovac, M. Sekulic, and B. Skoric, *J. Mech. Sci. Technol.* **26**, 173 (2012).
- [3] Z. Yu, K.P. Rajurkar, and J. Narasimhan, *ASPE Precis. Mach. Annu.* Portland, OR (2003).
- [4] M. Vulliez, M.A. Gleason, A. Souto-Label, Y. Quinsat, C. Lartigue, S.P. Kordell, A.C. Lemoine, and C.A. Brown, *Procedia CIRP* **13**, 308 (2014).
- [5] J. George and M. Chandrasekaran, in *Asp. Mech. Eng. Technol. Ind.* (Nirjuli, India, 2014), pp. 278–284.
- [6] A.A. Aliyu, A.M. Abdul-Rani, T.L. Ginta, C. Prakash, E. Axinte, M.A. Razak, and S. Ali, *Adv. Mater. Sci. Eng.* **2017**, (2017).
- [7] H. Ding, X. Li, X. Wang, L. Guo, and L. Zhao, in *Proc. 2nd Int. Conf. Adv. Mech. Eng. Ind. Informatics (AMEII 2016)* (Atlantis Press, Paris, France, 2016), pp. 1316–1320.
- [8] X. Yang, J. Guo, X. Chen, and M. Kunieda, *Precis. Eng.* **35**, 51 (2011).
- [9] J. Tao, J. Ni, and A.J. Shih, *J. Manuf. Sci. Eng. Trans. ASME* **134**, 1 (2012).
- [10] T. Bartkowiak and C.A. Brown, *J. Manuf. Sci. Eng.* **140**, (2018).
- [11] S. Arooj, M. Shah, S. Sadiq, S.H.I. Jaffery, and S. Khushnood, *Arab. J. Sci. Eng.* **39**, 4187 (2014).
- [12] ISO CD 25178-2:2012 “Geometrical Product Specification (GPS) – Surface Texture: Areal – Part 2: Terms definitions and surface texture parameters,” Geneva Int. Organ. Stand. (2012).
- [13] R. Laheurte, P. Darnis, N. Darbois, O. Cahuc, and J. Neauport, *Opt. Express* **20**, 13551 (2012).
- [14] J. Weingarten, *J. Für Die Reine Und Angew. Math.* **59**, 382 (1861).
- [15] M.A. Gleason, S. Kordell, A. Lemoine, and C.A. Brown, in *14th Int. Conf. Metrol. Prop. Eng. Surfaces, Taipei, Taiwan, Pap. TS4-01* (2013).
- [16] C.A. Brown, H.N. Hansen, X.J. Jiang, F. Blateyron, J. Berglund, N. Senin, T. Bartkowiak, B. Dixon, G. Le Goïc, Y. Quinsat, W.J. Stemp, M.K. Thompson, P.S. Ungar, and E.H. Zahouani, *CIRP Ann.* **67**, 839 (2018).